

Large Area Planar Cell Simulation Tool (DREAM SOFC-PC)

Jerry H. Mason^{1,2}, Ismail B. Celik^{1,3,5}, Hayri Sezer^{1,4,5}, Mohamed A. S. Zaghloul⁶, Mohan Wang⁶, Michael Buric¹, Zhaoqiang Peng⁶, Paul Ohodnicki⁶, Shiwoo Lee^{1,2}, Thomas Kalapos^{1,2}, Harry Abernathy^{1,2}, Kevin Peng Chen⁶, Gregory A. Hackett¹

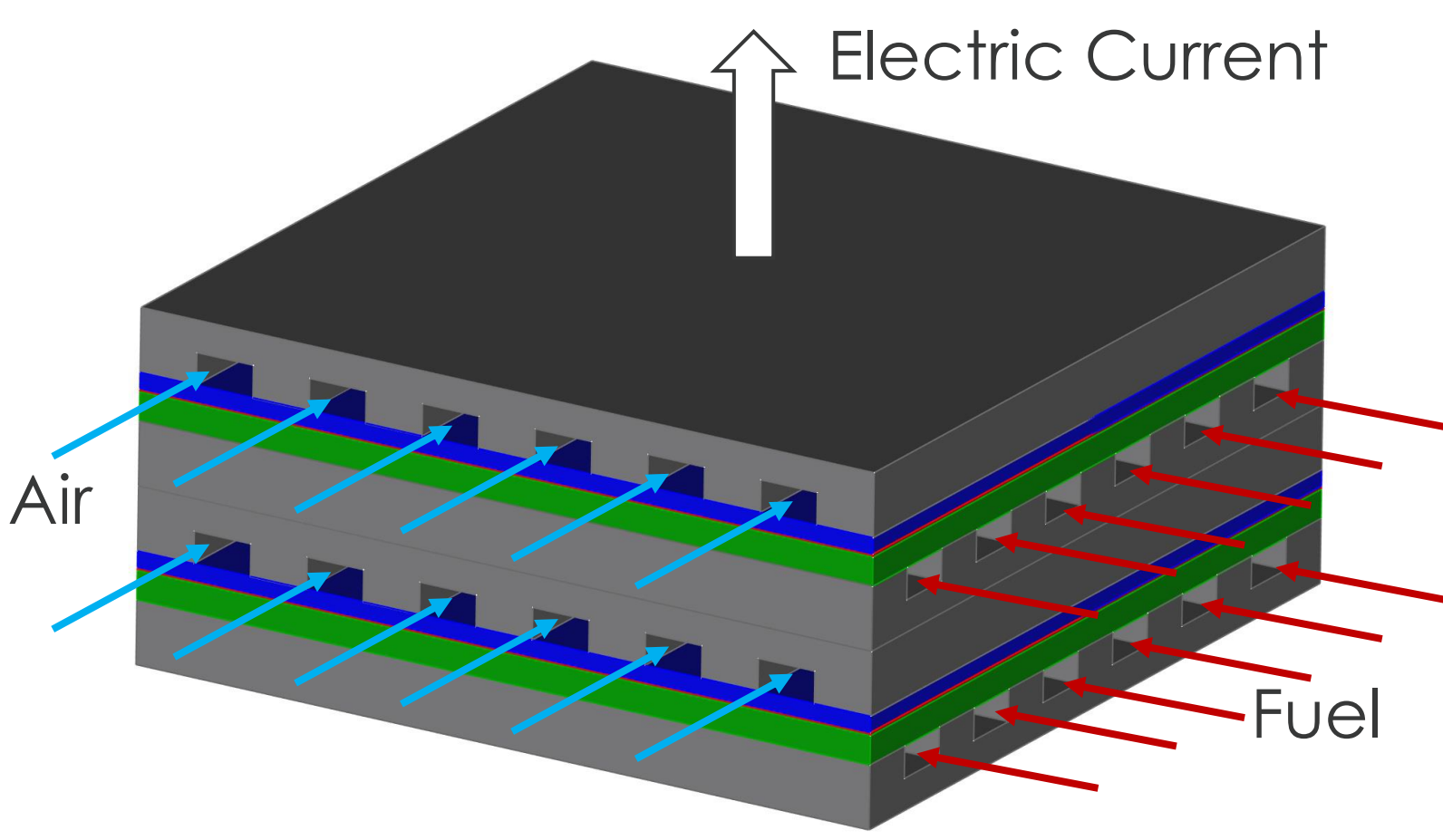
¹US Department of Energy, National Energy Technology Laboratory, Morgantown, WV/ Pittsburgh, PA/Albany, OR; ²Leidos Research Support Team, Morgantown, WV/ Pittsburgh, PA/Albany, OR; ³West Virginia University, Morgantown, WV; ⁴Western Carolina University, Cullowhee, NC; ⁵Oak Ridge Associated Universities, Oak Ridge, TN; ⁶University of Pittsburgh, Pittsburgh, PA

Research & Innovation Center



Summary

- In house code, **DREAM SOFC-PC** – applied to simulate performance of large area SOFCs
- Capable of simulating transient cell response, long term degradation and performance metrics of VI and impedance curves using the same simulation tool
- Automatic meshing routine allows for user input of channel and layer dimensions – including cross flow geometry
- Example applications to fuel contaminant degradation and study of the impact of optical fiber temperature sensors are highlighted



Model Equations [1,2]

General Transport equations (3D)

Equations solved via finite volume method throughout the domain using cell-IDs to determine property distributions and source terms

Gas species transport – solve for mass fraction of species j in the pore phase X_j^p :

$$\frac{\partial}{\partial t}(\epsilon_p \rho_p X_j^p) = \nabla \cdot (\epsilon_p \rho_p \nabla X_j^p) + \epsilon_p \rho_p S_j^p + f_{I,p,s}$$

Source term S_j^p includes chemical reactions (i.e. water gas shift, methane reforming) and interface flux $f_{I,p,s}$ calculated from Faraday's law.

Heat transfer – solve for enthalpy h , with the assumption that $dh = C_p dT$:

$$\frac{\partial}{\partial t}(\rho C_p T) + \nabla \cdot (\lambda \nabla T) + \rho S_h$$

Where source term S_h considers heat from Ohmic heating and reactions

Charge transport – derived from Ohm's law $\nabla \cdot \vec{I} = \nabla \cdot (\sigma \nabla \phi) = s = \nabla \cdot (\sigma \nabla (\phi - \eta_{act}))$

$$\eta_{act,j} = \frac{RT}{\alpha_j n_j F} \ln \left(\frac{i_j}{2i_{0,j}} + \sqrt{\left(\frac{i_j}{2i_{0,j}} \right)^2 + 1} \right)$$

$$i_{0,j} = c_j \left(\frac{Y_{j,int}}{Y_{j,ref}} \right) \exp \left(\frac{E_{j,act}}{RT} \right)$$

Gas channel model (1D)

Gas species transport – 1D Plug flow assumed in the fuel/air channels, reducing to:

$$\frac{\partial}{\partial t}(\rho A X_j) = -\frac{\partial}{\partial z}(A \rho v X_j) + \frac{\partial}{\partial z}(A D_{eff} \frac{\partial X_j}{\partial z}) - \dot{Q}_j$$

A is the channel cross section area and \dot{Q}_j is the flux across channel walls interfaces

Using mass transfer coefficient k_j as:

$$\dot{Q}_j = k_j A (X_{j,e} - X_{j,c})$$

Mass is balanced with by setting $r_{p,j}^{eff} = k_j \Delta y_{int}$ at the interface

Velocity is calculated assume constant pressure:

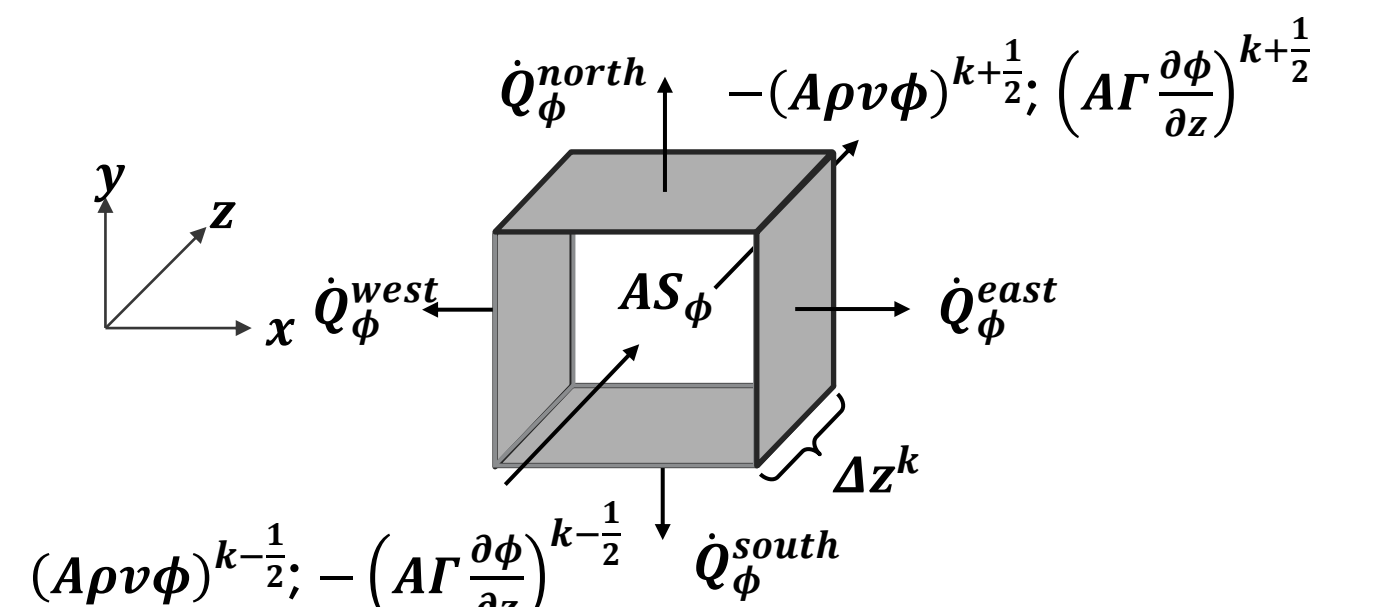
$$v_z = \frac{(\rho v)_z - \sum_j Q_j \frac{\Delta z}{\Delta V}}{\rho_z}$$

Heat Transfer – solve for the enthalpy h , with the assumption that $dh = C_p dT$:

$$\frac{\partial}{\partial t}(\rho A C_p T) = -\frac{\partial}{\partial z}(A \rho v C_p T) + \frac{\partial}{\partial z}(A \lambda \frac{\partial C_p T}{\partial z}) - \dot{Q}_h$$

Flux considers both heat transfer due to mass transport:

$$\dot{Q}_h = \sum_j C_{p,j} \dot{Q}_j T + \sum_m h_m A_m (T - T_m); \quad h_m = \frac{Nu \lambda_m}{D_h}$$



Meshing Routine

Algorithm uses maximum grid expansion ratio (r_{max}) to limit this ratio and iterative process to maintain proper boundaries between cell layers

$r = \frac{\Delta x_1}{\Delta x_{n_x}}$ - ratio between first and last grid size of a layer

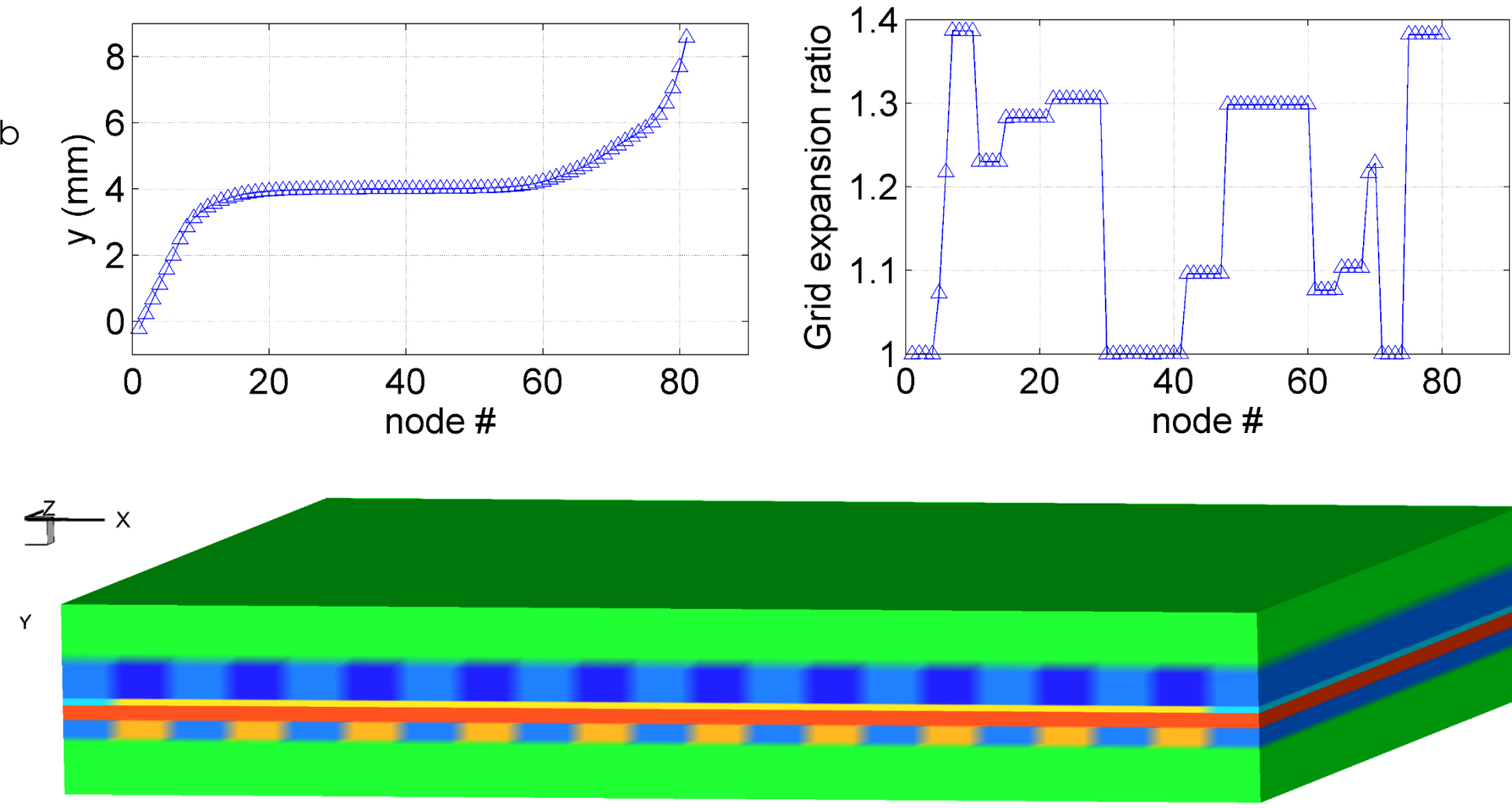
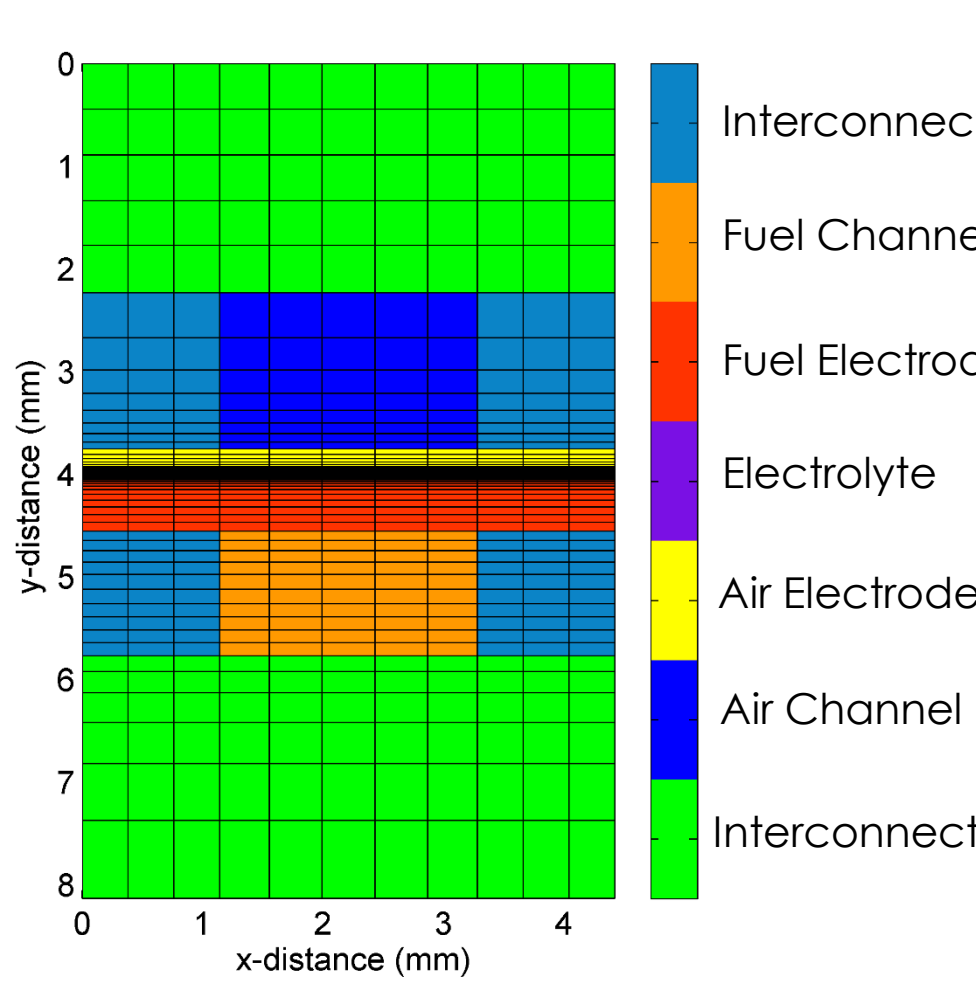
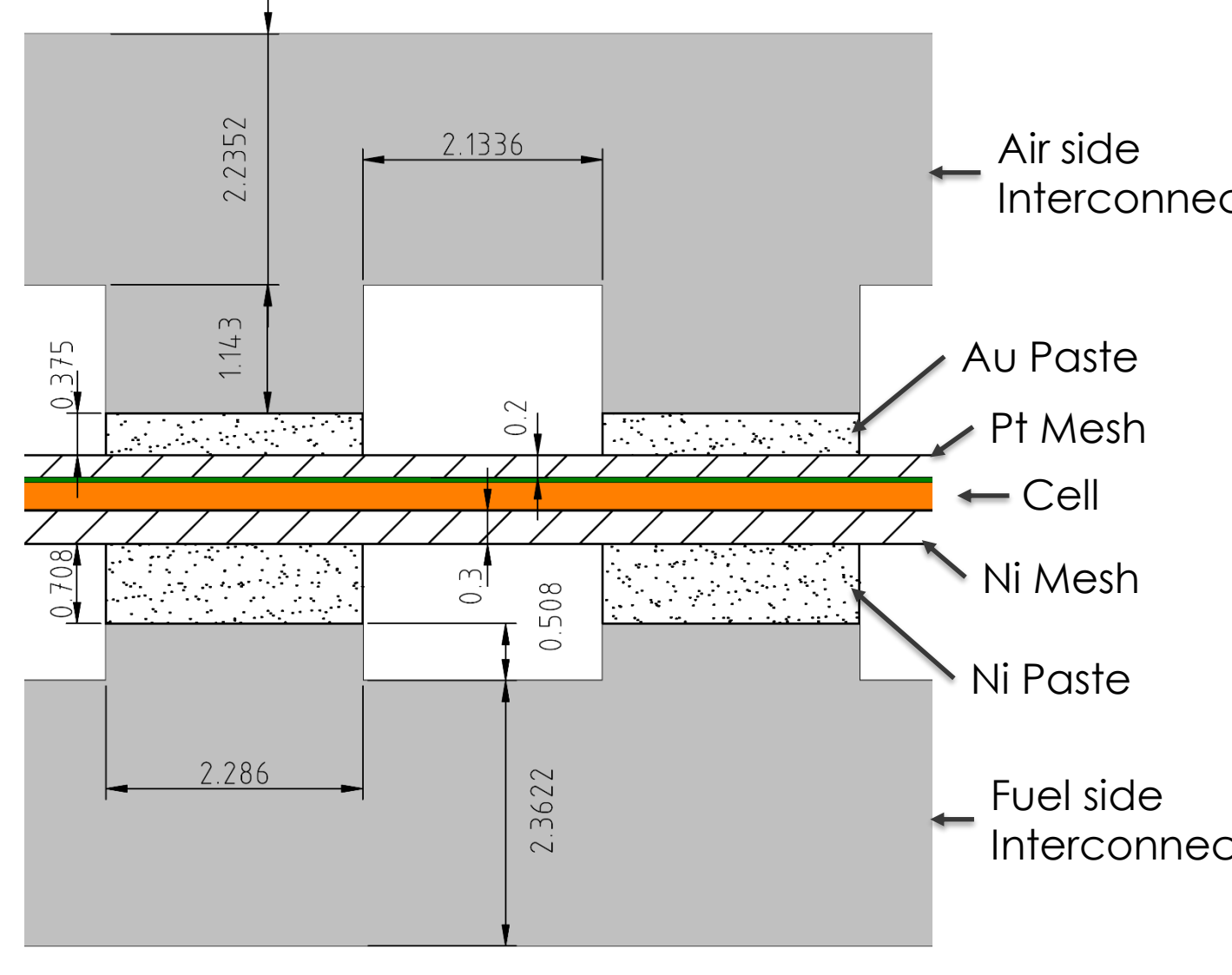
$n_x = 2 + \frac{\ln(r)}{\ln(r_{max})}$ - minimum number of grid points in layer

$r_{new} = \frac{1}{r_{old}^2}$ - actual grid expansion ration

$x^i = x^{i-1} + r_{new}^{i-1} \Delta x_i$ - produce grid layer ($i = 2$ to n_x)

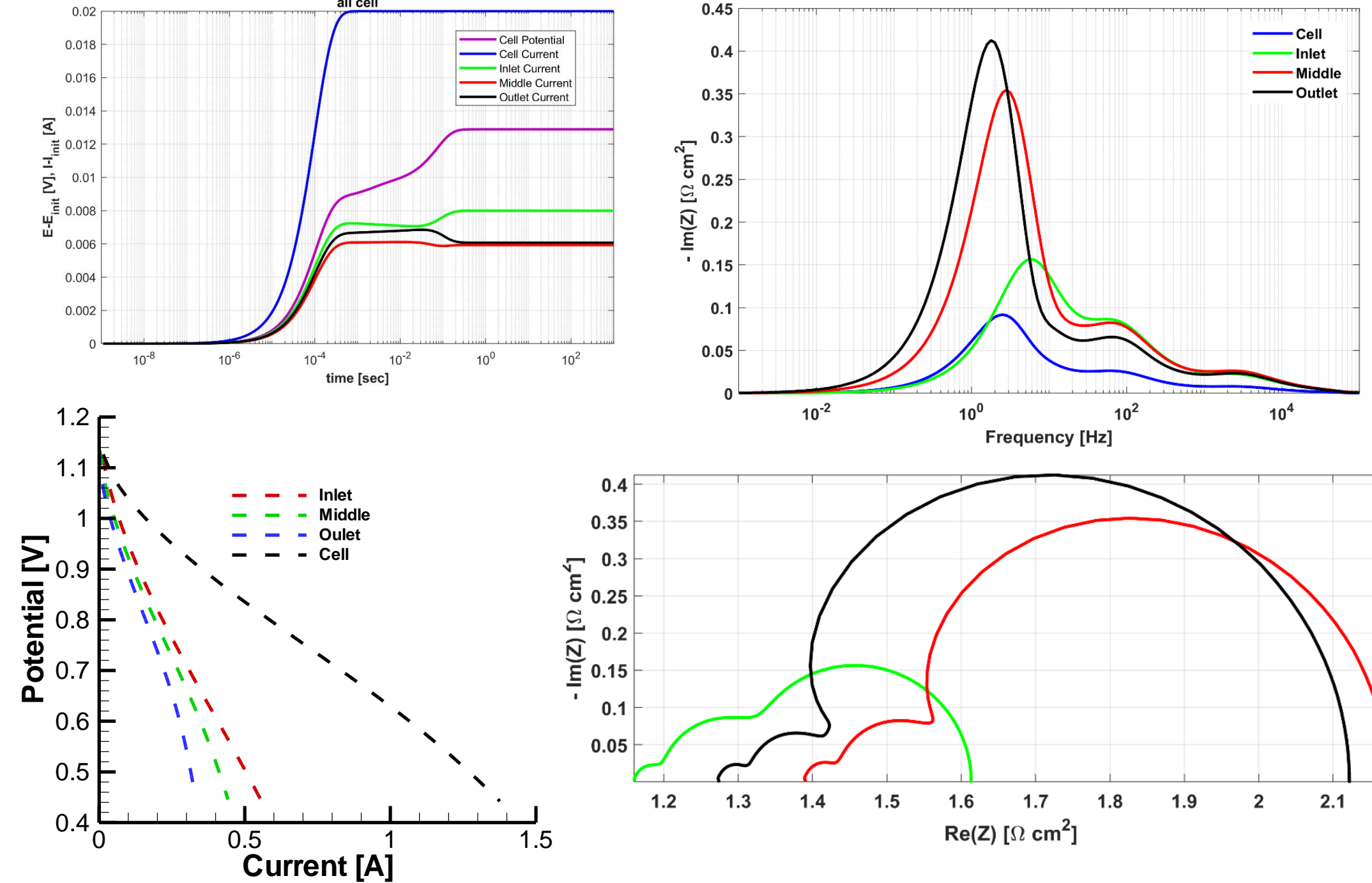
- Repeat for each layer from smallest grid size to largest

Example: Cell with 250 μm fuel electrode with 10 μm active layer, 40 μm air electrode with 5 μm active layer and 5 μm electrolyte with set up shown to the right



Performance Evaluation Metrics

- VI Curve** produced by holding either current or potential constant, scanning through applied loads at user input interval
- Impedance curve** produced using current interruption method (Bessler [3]) applying interpolation in frequency space
- Location dependent performance** obtained by considering cell sections independently

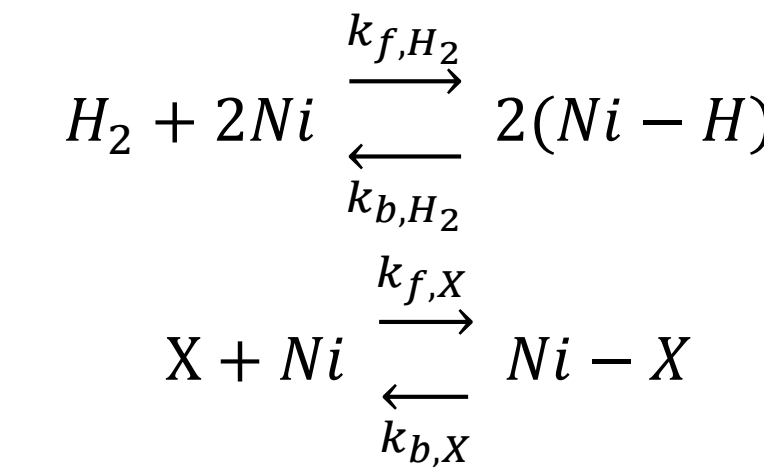


Application I: Degradation due to fuel contaminants [4][5]

Model assumptions:

- Impurity molecules chemically react to form secondary phases, these secondary phases (contaminant coverage) are assumed to block the active sites of catalytic material.
- Decreases the reaction rate of the half cell reaction

Monolayer adsorption mechanism



- Contaminant coverage and secondary phase formation is believed to block pores
- Decreases the effective diffusion of the fuel
- Decreases the reaction rates of the half cell reaction

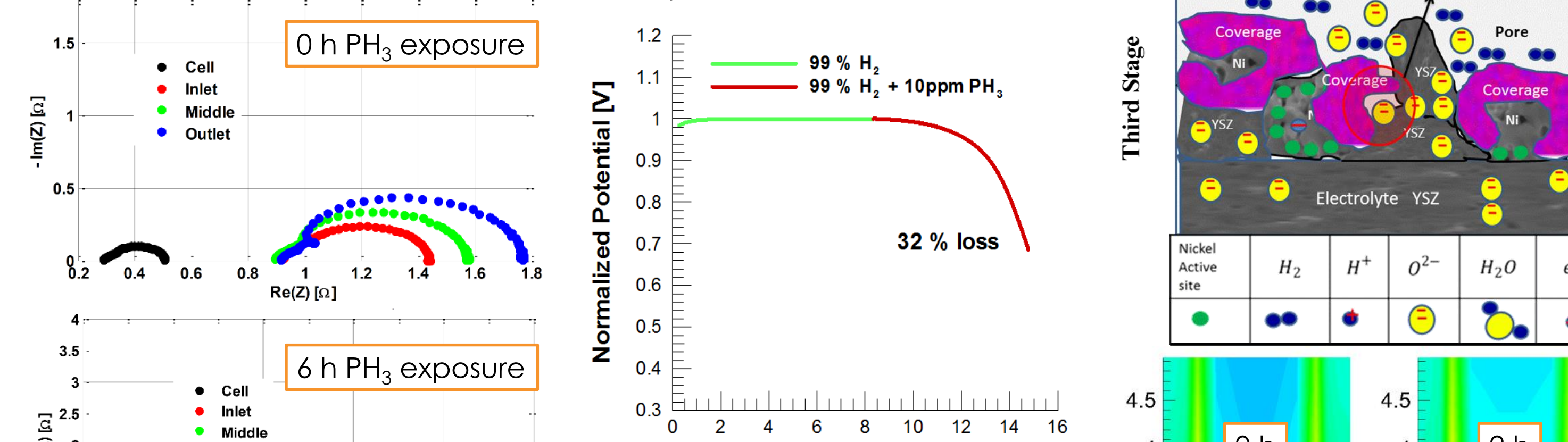
Transport of surface coverage

$$\frac{\partial \theta_i}{\partial t} = D_\theta \nabla^2 \theta_i + \omega_{\theta_i}$$

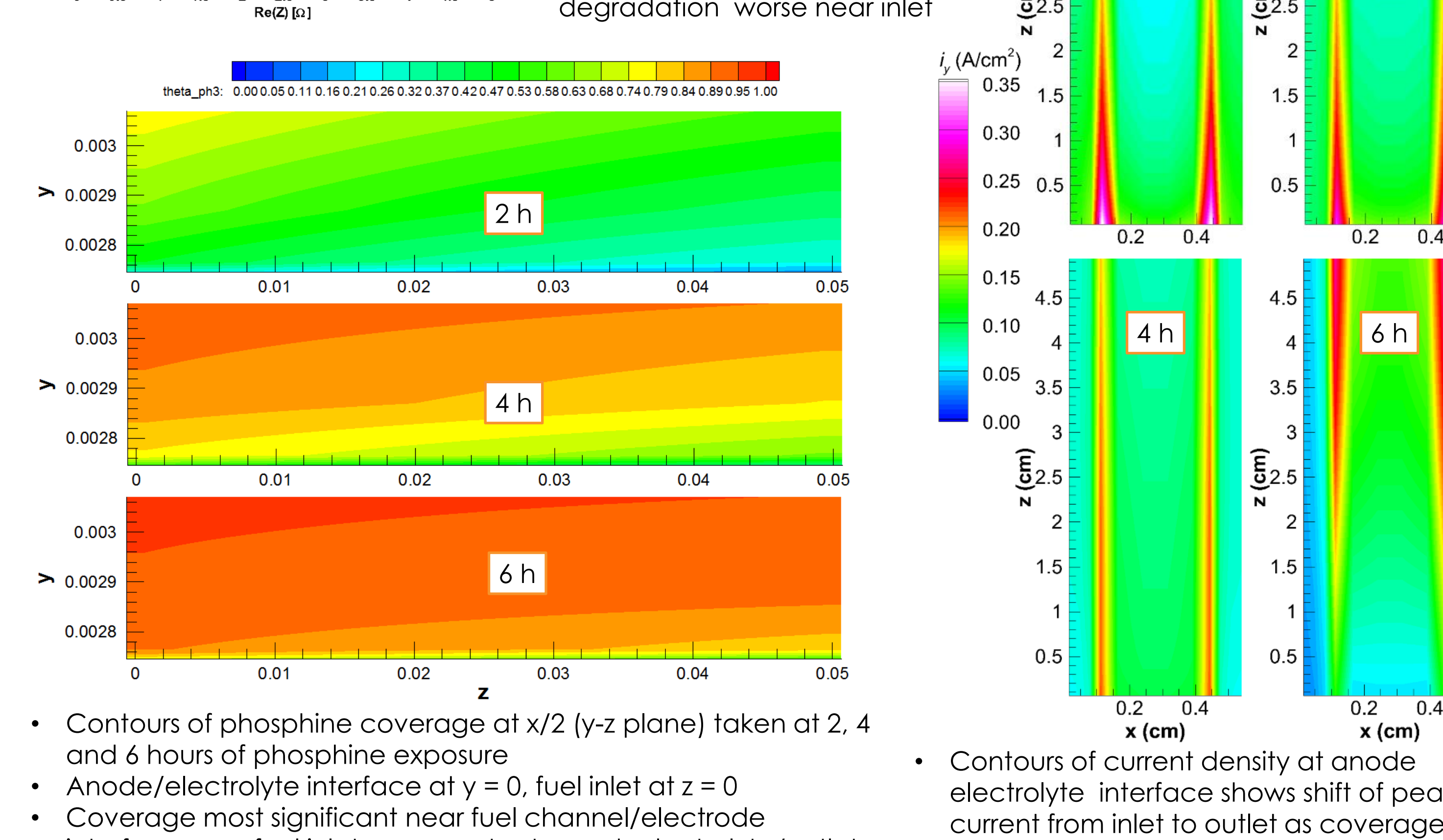
$$\theta_{Ni-X} + \theta_{Ni-H} + \theta_{Ni} = 1$$

$$\omega_{\theta_X} = k_{f,X} Y_X \theta_{Ni} - k_{b,X} \theta_{Ni-X}$$

$$\omega_{\theta_{Ni-X}} = k_{f,H} Y_{H_2} \theta_{Ni}^2 - k_{b,X} \theta_{Ni-X}^2$$



Cell voltage drops ~32% during phosphine exposure
Location specific analysis shows degradation worse near inlet

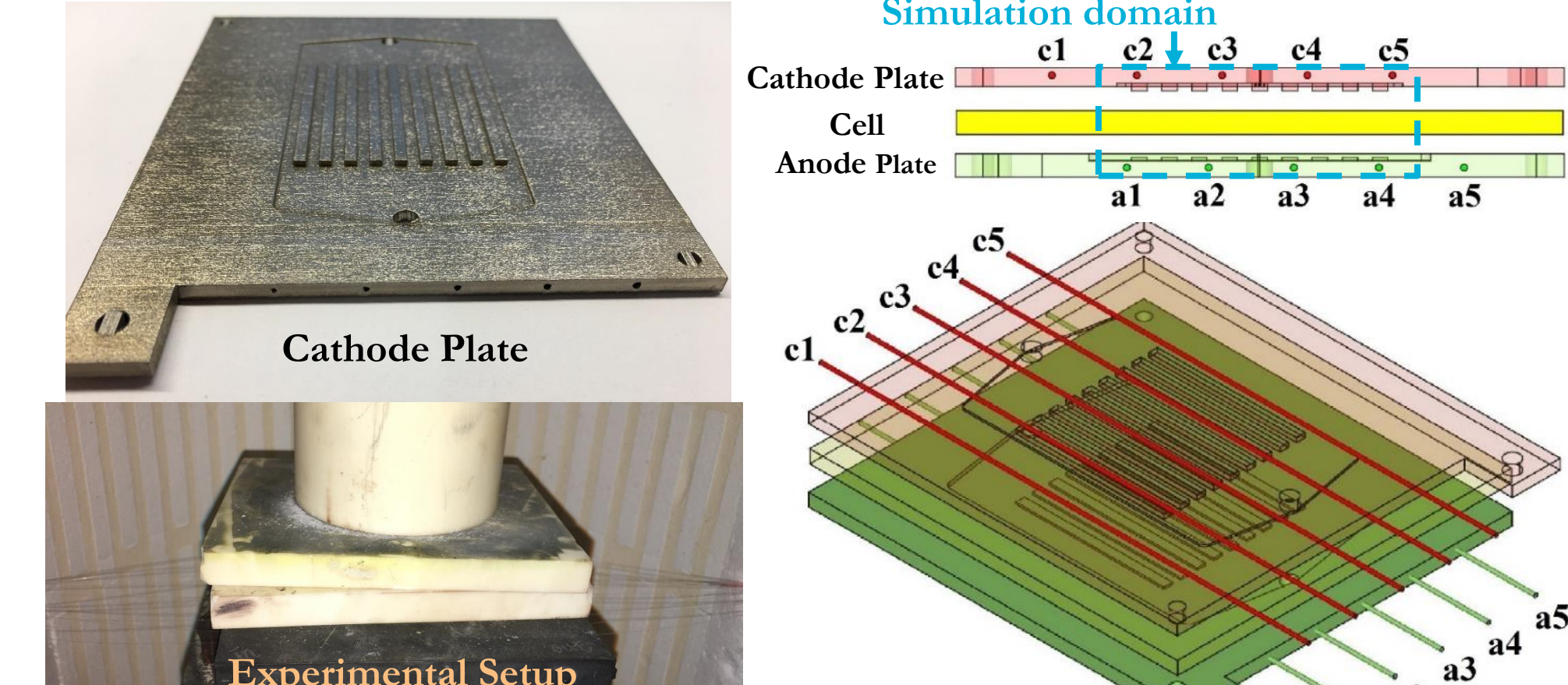


- Contours of phosphine coverage at $x/2$ ($y-z$ plane) taken at 2, 4 and 6 hours of phosphine exposure
- Anode/electrolyte interface at $y = 0$, fuel inlet at $z = 0$
- Coverage most significant near fuel channel/electrode interface near fuel inlet, propagates towards electrolyte/outlet
- Contours of current density at anode electrolyte interface shows shift of peak current from inlet to outlet as coverage promulgates

Application II: Optical fiber sensors [6]

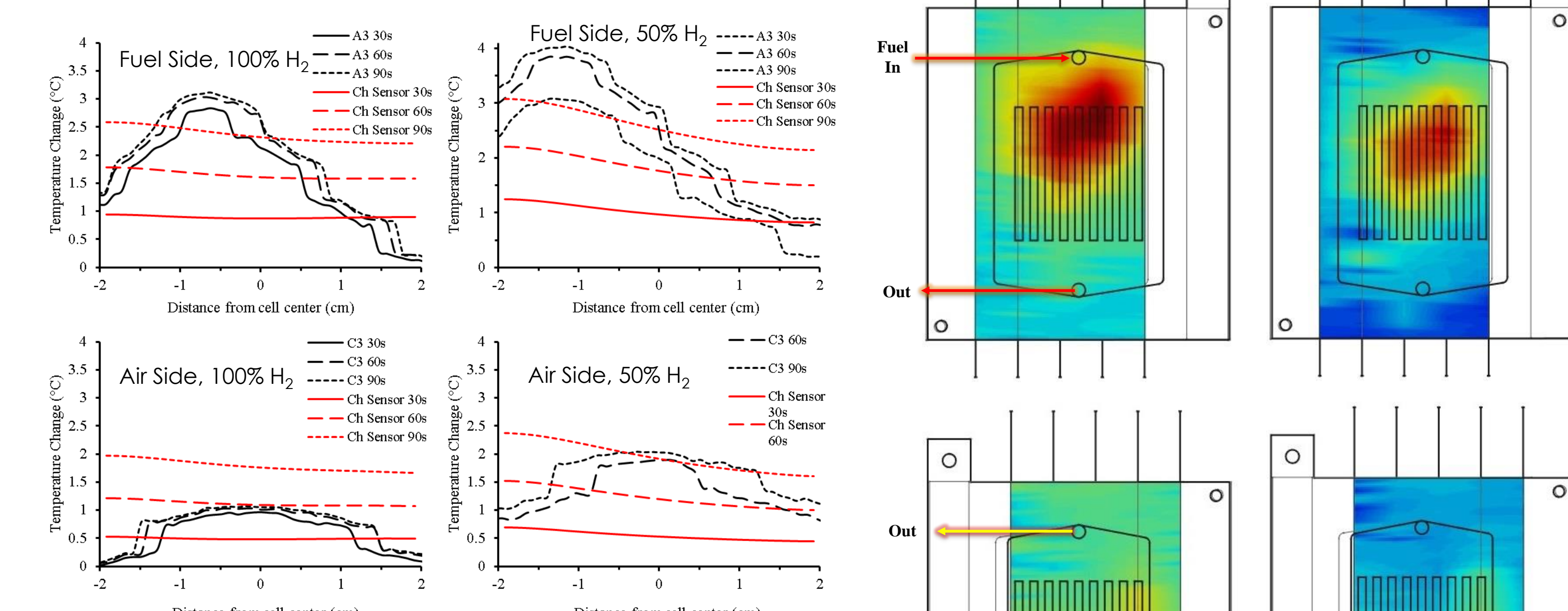
Experiment

- Current collector plates 3D printed with 750 μm holes for sensors
- Femtosecond laser irradiation to stabilize Rayleigh scattering profile
- Measurements with ~4 mm spatial, ~0.1°C temperature resolution
- Cell operated at 750°C, 100 sccm flow rates for fuel and air, counter flow
- Temperature transients measured during first 90s of applied current, different fuel mixtures compared

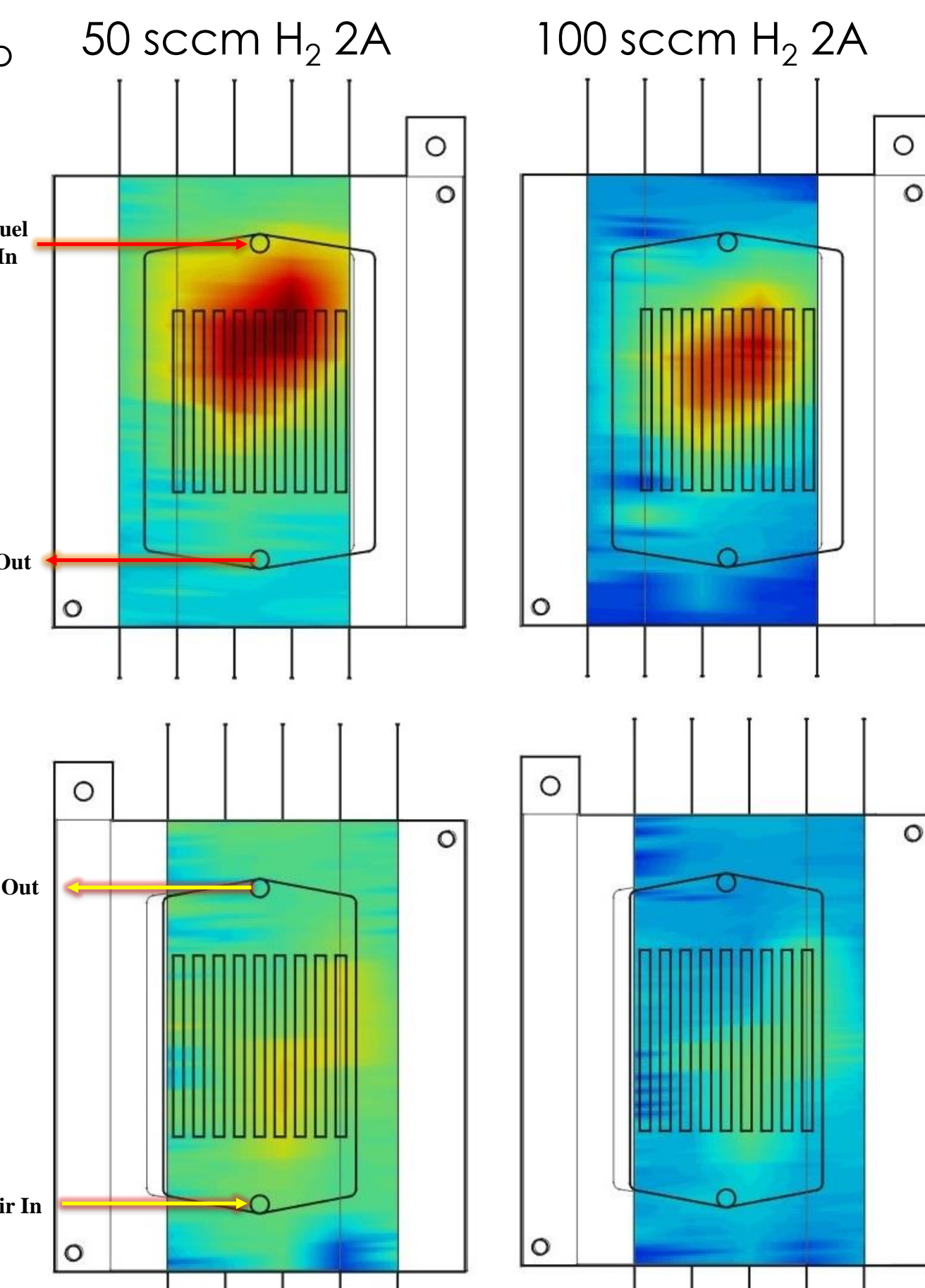


Model

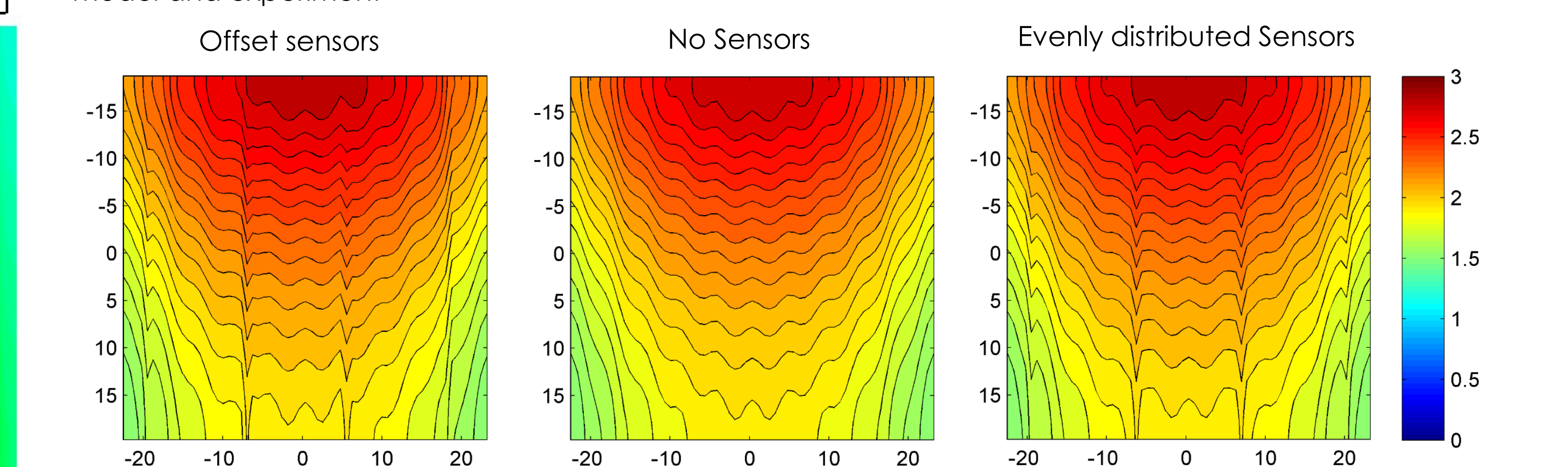
- Single channel simulations with sensors located adjacent to rib and channel as well as full cell simulations performed
- Sensor modeled as an air gap



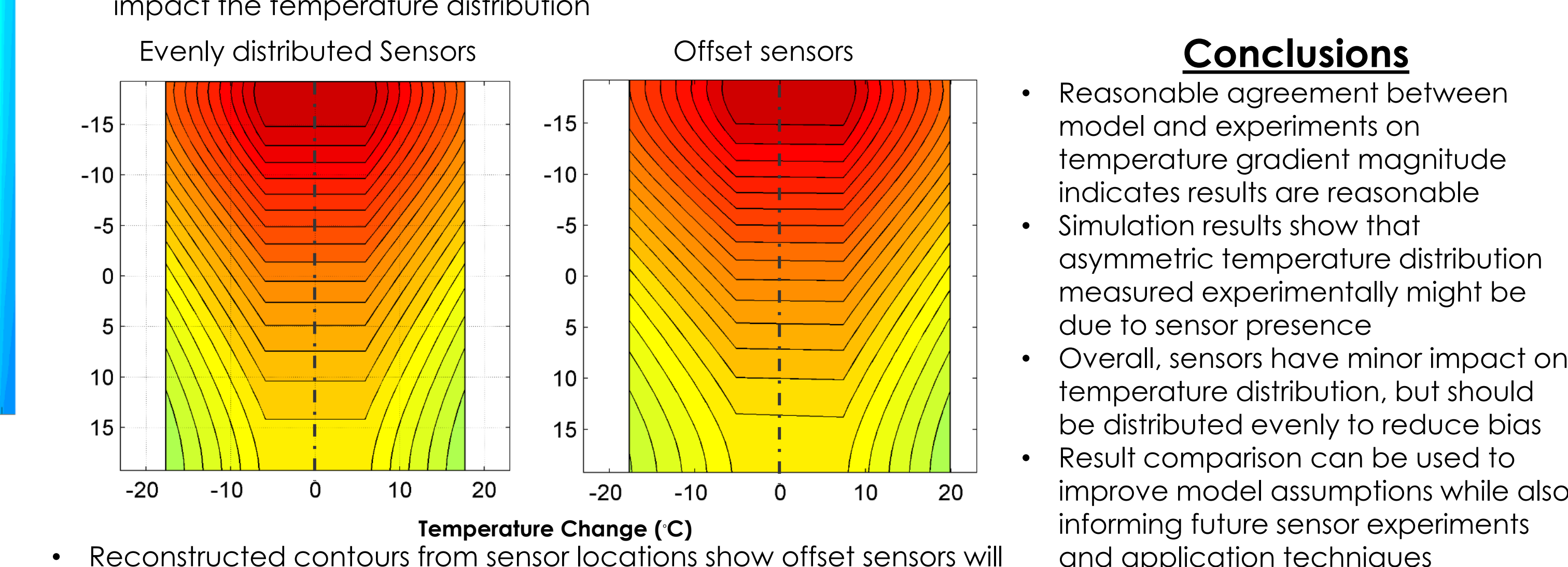
- Temperature distributions plotted from the anode, and cathode sensors a3 and c3, respectively. Model results in red, experiments in black
- The peak on the anode side, appears closer to the H_2 gas inlet and shifts closer to the fuel inlet as the H_2 flow rate is reduced.
- Cathode side temperature ~1°C lower, peak in the center from experiment, toward fuel inlet in the simulations
- Highest peak 50% molar H_2 case (~4°C in experiment, ~3°C in simulation)
- Overall, temperature magnitudes similar between model and experiment



- 2D temperature contours constructed for anode (top) and cathode (bottom) from sensor data (90 s data shown here)
- Peak temperature occurs near cell center, fuel inlet, **contour is skewed to one side** consistently



2D temperature contours from full cell simulations (50 sccm H_2 /50 sccm N_2 case at 90s) show sensors will impact the temperature distribution



Conclusions

- Reasonable agreement between model and experiments on temperature gradient magnitude indicates results are reasonable
- Simulation results show that asymmetric temperature distribution measured experimentally might be due to sensor presence
- Overall, sensors have minor impact on temperature distribution, but should be distributed evenly to reduce bias
- Result comparison can be used to improve model assumptions while also informing future sensor experiments and application techniques



References:
[1] S.R. Kalogirou, A new reduced order model for solid oxide fuel cells, (2006).
[2] F. Elizalde-Blanco, Modeling issues for solid oxide fuel cells operating with coal syngas, (2009).
[3] W. G. Bessler, J. of ECS, 154(11) (2007), 1186-1191
[4] F.N. Gayen, et al., Fuel Cells, 12 (2012), 464-473
[5] H. Sezer, Refined computational modeling of SOFCs degradation due to trace impurities in coal syngas, (2014)
[6] Buric, M., et al, Remote Sensing System Engineering VI, 9777 (2016), Int. Soc. for Optics and Photonics.

Acknowledgment: Research performed by Leidos Research Support Team staff was conducted under the RSS contract 89243318CFE00000. Supported in part by an appointment to the NREL Research Participation Program, sponsored by the U.S. Department of Energy and administered by the Oak Ridge Institute for Science and Education. Research performed by the University of Pittsburgh was supported by the Department of Energy under Grants DE-FC031175 and DE-DE0002892.
Disclaimer: Neither the United States Government nor any agency thereof, nor any of their employees, nor LRSI, nor any of their employees, makes any warranty, expressed or implied, or assumes any legal liability or responsibility for the accuracy, completeness, or usefulness of any information, apparatus, product, or process disclosed, or represents that its use would not infringe privately owned rights. Reference herein to any specific commercial product, process, or service by trade name, trademark, manufacturer, or otherwise, does not necessarily constitute or imply its endorsement, recommendation, or favoring by the United States Government or any agency thereof. The views and opinions of authors expressed herein do not necessarily state or reflect those of the United States Government or any agency thereof.

Science & Engineering To Power Our Future